CFD INVESTIGATION OF THE IMPROVEMENT OF SMOKE CONTROL IN A TUNNEL EQUIPPED WITH A LONGITUDINAL AND A TRANSVERSE VENTILATION SYSTEM

[1]Gabriel Remion, [1]Antoine Mos, [2]Pietro Salizzoni, [2]Massimo Marro, [2]Stefano Lanzini
[1]Center for Tunnel Studies (CETU), FR
[2]Laboratoire de Mécanique des Fluides et Acoustique (LMFA), FR

DOI 10.3217/978-3-85125-996-4-36 (CC BY-NC 4.0)

ABSTRACT

Smoke control in the case of a tunnel fire is vital to ensure an atmosphere allowing tunnel users to evacuate. Depending on the type of ventilation, namely the longitudinal or the transverse ventilation system, the aim is respectively either to push the smoke longitudinally towards a tunnel exit or to evacuate the smoke transversally by the tunnel ceiling. In France, the regulation imposes a sufficient mechanical airflow to prevent any smoke back-layer and to ensure an efficient smoke exhaust.

Previous experiments implemented in a small-scale tunnel have shown the potential of solid barriers, or containment screens, attached to the tunnel's ceiling. The shape of dampers of the transverse ventilation strategy was also questioned. Wide rectangular dampers appeared to be significantly more efficient than narrower or square dampers, which are commonly installed. Both technical propositions increased significantly the robustness of both ventilation systems by reducing the airflow required to prevent any smoke back-layer from occurring. Reducing the required airflow goes along with reducing the power need of the ventilation system. It tackles the issues of energy consumption and the improvement of the robustness of existing ventilation systems. It also eases the dimensioning and cost of ventilation systems installed in new tunnels.

In the present work, a numerical Computational Fluid Dynamics model of those experiments has been validated by comparison with experimental data measured in both tunnel configurations. The StarCCM+ software was used. It allowed verifying numerically significant benefits of solid barriers for the longitudinal ventilation system. Regarding the transverse ventilation system, it also verified its increased robustness allowed by rectangular dampers compared to commonly used square dampers. The validation of this numerical model is a first step in a wider work aiming at numerically testing the equipment in other configurations.

Keywords: Tunnel, ventilation system's optimization, dampers' shape, containment screens, CFD

1. INTRODUCTION

In France, fire safety regulations impose every new tunnel longer than 500 m, or 300m in urban areas, to have a smoke exhaust ventilation system. Smoke exhaust is either achieved thanks to a longitudinal or a transverse ventilation system. Both systems should meet minimum performance requirements in order to ensure a safe auto-evacuation.

The first strategy is based on inducing a longitudinal airflow thanks to fans installed in the cross section of the tunnel, usually near the ceiling. The smoke is evacuated following the airflow towards the tunnel exit. The effectiveness of this strategy depends on the speed of the

longitudinal airflow. Below a threshold value, namely the critical velocity, there is a risk that a part of the smoke layer moves against the airflow. This phenomenon is called smoke back-layering. When the smoke back-layer is still near the fire, its temperature is still high and buoyancy forces maintain the smoke back-layer near the ceiling. The self-evacuation is not perturbed. However, after some distance from the fire, the smoke back-layer starts to decrease in temperature, and buoyancy forces become weaker. The smoke reaches lower zones of the cross section, which may prevent the auto-evacuation. Smoke back-layering may occur over long distances from the fire, which may significantly alter the safety level of the tunnel. An effective longitudinal smoke exhaust strategy relies on the absolute absence of the so-called smoke back-layer provided by a sufficiently high airflow (greater than the critical velocity).

The second strategy uses dampers located on the tunnel ceiling near the fire location to exhaust the smoke. Dampers are distributed all along the tunnel at specific interval (usually 50 to 100 m). The air is extracted thanks to fans that are located in a specific ventilation facility. Fans are then connected to dampers by a ventilation duct. The air is usually extracted through the closest 5 to 7 dampers from the fire location. The objective is to confine the smoke between the two extreme dampers from which the smoke is expected to be extracted. Similarly to the longitudinal strategy, a back-layer can occur. In this case, the back-layer is defined as a smoke layer moving upwind the confinement zone. To prevent the back-layer, the airflow flowing inside the tunnel (or similarly the airflow extracted by dampers) has to be higher than a threshold value called the confinement velocity.

Previous experiments implemented in a small-scaled tunnel located at the Fluid Mechanics and Acoustics Laboratory, in Centrale Lyon France, have tested several configurations to improve the efficiency of both aforementioned ventilation systems [1], [2]. Chaabat et al. [1] questioned the interest of implementing solid barriers, also called containment screens, in the cross section of the tunnel near the ceiling to improve the robustness of longitudinal ventilation systems. They found that containment screens allowed to significantly decrease the critical velocity up to 45%, i.e. the velocity which prevents smoke back-layering in longitudinal ventilation systems. Regarding transverse ventilation systems, Chaabat et al. [2] questioned the shape of dampers. A wide, "slit-like" rectangular damper appeared to be a lot more efficient than the usually implemented square damper located at the ceiling corner. The confinement velocity was decreased by 80%. Thus, significant robustness improvements were identified for both ventilation strategies. Those results are interesting because they allow to ease the dimensioning and the cost of new tunnels. It would also allow to improve the efficiency of already installed ventilation systems without replacing fans that can be very costly.

This paper presents a CFD model of these experiments. A comparison of results obtained experimentally and numerically is systematically performed. The aim is to give more credits to interesting results found experimentally. Section 2 presents the method. Section 2.1 describes configurations that were tested experimentally and reproduced numerically, and section 2.2 focuses on the implementation of the CFD model. Then, results are presented in section 3, first focusing on the contribution of barriers (section 3.1), and then on the influence of damper shapes (section 3.2).

2. METHODS

2.1. Tested configurations

Configurations that were tested experimentally, and that are reproduced numerically here, are presented in this section. Figure 1 shows a picture of the experimental set up of the transverse ventilation system. The small-scaled tunnel, which hosted experiments, is 8.4 m long, 0.18 m

high (H) and 0.36 m wide, around 1/25 of a real tunnel. The fire-induced smoke is reproduced by the injection of a light gas composed by a mixture of air and helium. This technique intends to simulate the smoke buoyancy while bypassing the influence of heat transfer, which is complicated to account for. Densimetric plumes have already been shown reliable in describing the behavior of fire-induced smoke in tunnels [3]. The buoyant source is located in the center of the tunnel, and is released through a circular hole 10 cm in diameter (D). The density ratio ρ_0/ρ_i between the ambient air, and the light gas was set to 0.7. Its influence was shown to be negligible by Salizzoni et al. [4].Varying the speed of injection of the light gas (W_i), several heat release rates could be simulated, which can be characterized by the plume Richardson number (Γ_i):

$$\Gamma_i = \frac{5}{16\,\alpha}\frac{(\rho_0 - \rho_i)\,g}{\rho_0}\frac{D}{{W_i}^2}$$

With $\alpha = 0.12$, the reference entrainment coefficient [5]. Richardson numbers of 2, 4, 6, 8 and 10 were tested, characterizing plumes more and more dominated by buoyancy forces instead of momentum.

The Froude number is introduced, and represents a dimensionless form of the longitudinal velocity. The Froude number is defined as the ratio between inertia forces induced by the longitudinal airflow, and buoyancy forces introduced by the buoyant source (with Bi the buoyancy flux).

$$Fr_{cr} = \frac{U_{0_{cr}}}{\left(\frac{B_i}{H}\right)^{1/3}}$$

A similarity analysis developed in several articles [2], [4] concluded that the critical or the confinement Froude number did not show any dependence on single buoyant source parameters for highly buoyant sources, meaning for high values of Γ_i. In other words, conclusions are independent from the heat release rate for highly buoyant sources.

Both ventilation systems were implemented. A fan was used to impulse the airflow of the longitudinal ventilation system. The transverse ventilation system was realized thanks to two dampers located symmetrically from the buoyant source, at a distance of 5H. Dampers were connected to an extraction fan located outside of the tunnel section. Extracting the air through these dampers induces a convergent airflow entering the tunnel symmetrically by both exits.

Barriers were implemented in the cross section of the tunnel, attached to the ceiling. Their width are equal to the width of the tunnel. Different heights were considered: two large barriers with a height of H/3 and H/4, and a small barrier with a height of H/10. Large barriers were located just upstream the source of the fire. In configurations testing small barriers, one was also placed just upstream of the source but several other barriers were distributed all along the tunnel, with a fixed spacing of H between each other. Figure 2 shows those two configurations (schematics a. and b.).

Regarding the transverse ventilation system, three different shapes were tested: the usual square shape (0.104 m x 0.104 m) located in the center of the ceiling (SSD – PC), the square shape located in a corner of the ceiling (SSD – PS), and a narrow rectangular shape (0.32 m x 0.034 m) whose width is almost equal to the width of the tunnel (RSD). Figure 2 also presents these configurations (schematics c.).

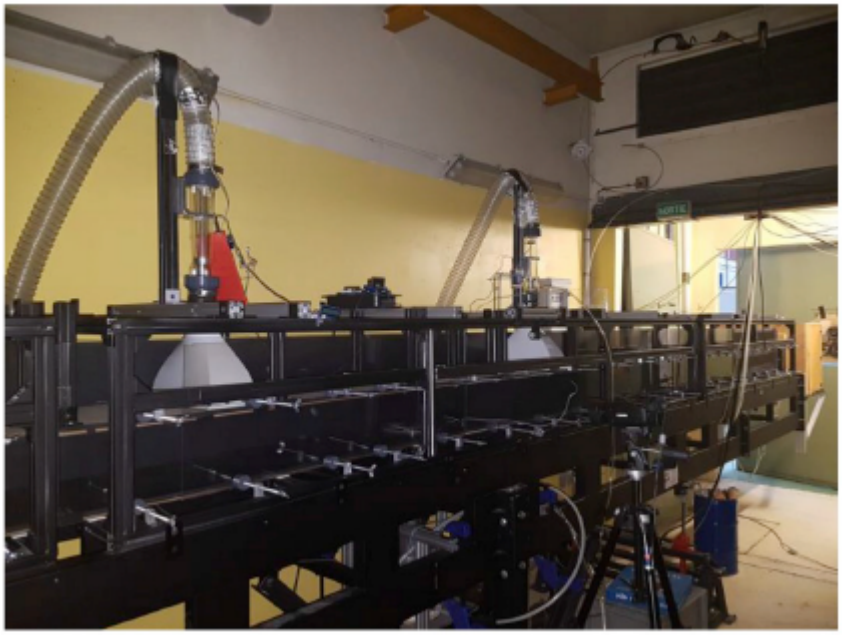

Figure 1: Picture of the experimental set up for the transverse SSD - PC ventilation system

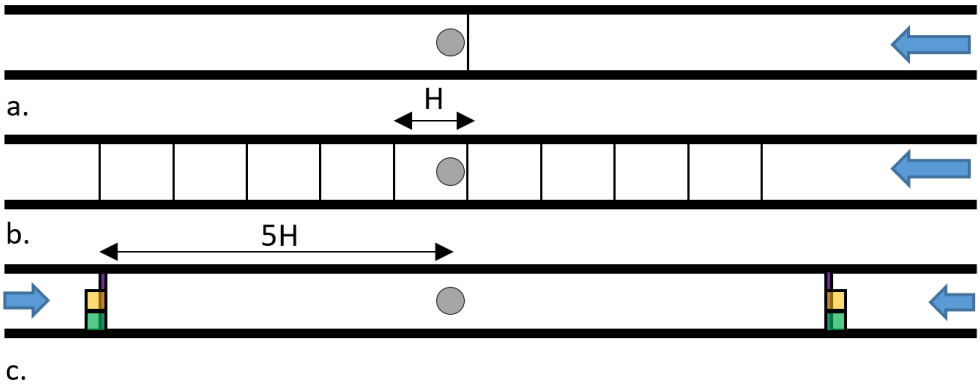

Figure 2: Schematics of configurations: a. longitudinal system with large barriers; b. longitudinal ventilation system with small barriers; c. transverse ventilation system with SSD - PC (yellow squares), SSD - PS (green squares), RSD (purple rectangles)

2.2. CFD model

The experimental set up presented in the previous section was modelled using the StarCCM+ CFD software. An isothermal steady RANS realizable k-epsilon closure model was implemented. Regarding the longitudinal ventilation system, the inlet of the tunnel was imposed as a constant velocity inlet on the cross section of the tunnel. The turbulence intensity and the turbulent length scale were defined in accordance with standard values for rectangular ducts. The exit was defined as a pressure outlet.

The air extracted from dampers of the transverse ventilation system was done by a mass flow inlet boundary condition. Both tunnel's exits from which the convergent airflow enters the tunnel were defined as pressure outlets, meaning that a reversed flow occurs. Those boundary conditions were expected to be the most representative of the real physics.

For both configurations, the buoyancy source was introduced as a mass flow inlet of the same mixture of Air and Helium. Authors made sure that the length between tunnel's exits and the zone of interest allowed a well-established boundary layer.

The mesh is generated by the trimmed mesher provided by StarCCM+, which is particularly suited to tunnel applications with longitudinal airflows. Prismatic layers were defined on walls and barriers to ensure the low-Reynolds resolution (y+ ~ 1). The mesh grid represents 100k to 1 million cells depending on configurations. Authors made sure that results were independent from a mesh refinement.

3. RESULTS & DISCUSSION

3.1. Effect of barriers on the performance of longitudinal ventilation system

To obtain critical velocities, the inlet velocity was iteratively reduced until Helium was detected upstream of the extremity of the buoyant source (or upstream of the barrier). Figure 3 shows a smoke back-layer, which occurred in the configuration with a large H/3 barrier. The critical velocity found for a Richardson number $\Gamma_i = 2$ is about 0.155 m/s.

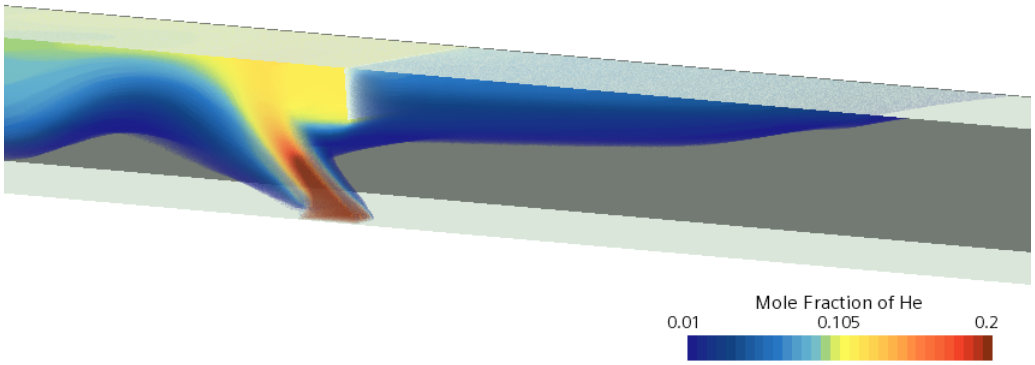

Figure 3: Configuration with barrier H/3 with a smoke back-layer occurring for critical velocity of 0.155 m/s, and Richardson number of 2

Figure 4 shows the dimensionless critical velocity in the form of the critical Froude number. It is plotted against the Richardson number for each configuration. Triangles, solid and dashed bars refer respectively to simulation results, experimental and simulation best fits. Best fits (experimental and simulation) were applied on critical Froude numbers obtained for $\Gamma i > 8$, as the behavior of the Froude number seem to be different on both sides of this threshold value. As was stated on section 2.1, the critical Froude number is expected to be independent from buoyant source parameters as long as the buoyant source is buoyant enough. Yet, for small Γ_i, ($\Gamma_i < 8$) the critical Froude number seems to increase with increasing Γ_i, whereas for higher values of Γ_i, ($\Gamma_i > 8$), it becomes constant. It was already observed experimentally [2], and this is consistent with findings presented in ref. [2], [4], that show a constant critical Froude number for high values of Γ_i. It can be noted that, even for small values of Γ_i , the evolution of the critical Froude number with Γ_i is quite similar for each configuration. Benefits allowed by barriers are, thus, independent from the heat release rate of the fire.

Before focusing on benefits allowed by barriers, it is interesting to compare experimental and simulation results. Indicative 10% error bars were added to simulation results. The reference configuration with no barriers shows an underestimation of simulation results. The deviation decreases as Γ_i increases, and lies below 10% from $\Gamma_i = 20$. The average underestimation is about 8% (0.017 m/s). Small barriers *H*/10 show good correlations. Finally large barriers lead to an overestimation compared to simulation results. The average deviation of large barriers *H*/4 and *H*/3 is respectively 13% (0.012 m/s) and 10% (0.017 m/s). In general, deviations

between experimental and simulation results are all within 13% (0.017 m/s), which demonstrates a rather good correlation.

We now focus on benefits brought by barriers. As critical Froude number and velocity are proportional, benefits observed on critical Froude numbers are equivalent to those on critical velocities. Focusing on simulation results, small barriers allow a small benefit of 3%. Considering the confidence interval, this benefit is insignificant. However, large barriers allow a significant reduction of the critical velocity. Large barriers *H*/4 and *H*/3 allow to reduce the critical velocity by respectively 22%, and 33% on average.

Experimental results showed also a rather small benefit of small barriers, but greater benefits of large barriers. Barriers *H*/4 and *H*/3 led to a reduction of the experimental critical velocity of respectively 35% and 45% (compared to 22% and 33% numerically). Those results show that both investigation techniques demonstrated significant benefits of large barriers in reducing the velocity that prevents any smoke back-layer to occur.

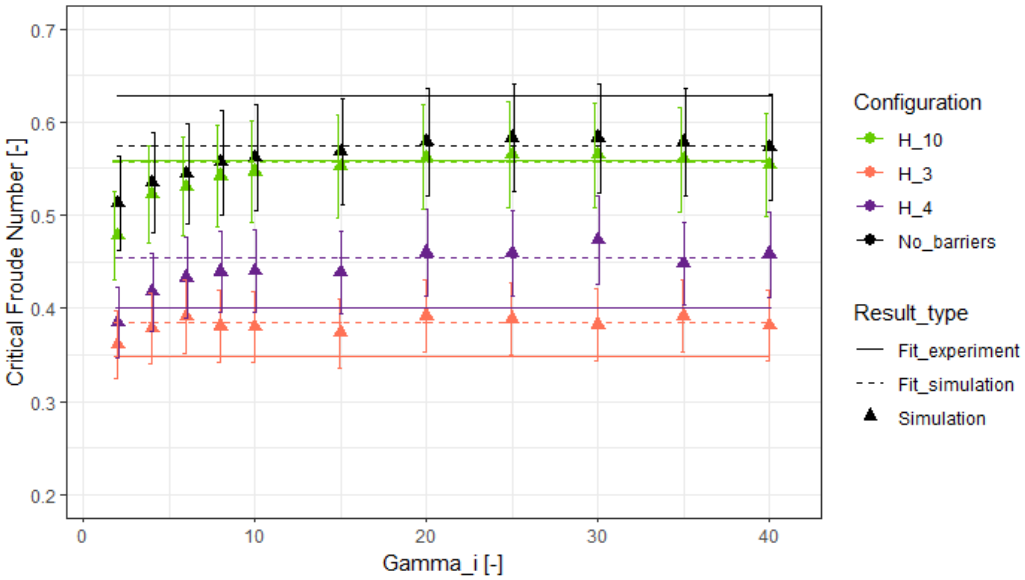

Figure 4: Froude number plotted against the Richardson number for each configuration

3.2. Effect of dampers' shape on the performance of transverse ventilation system

The influence of dampers' shape is questioned in this paragraph. The confinement velocity was assessed by iteratively reducing the extracted air flow rate until helium was detected upstream of the dampers (the flow is symmetrical). Figure 5 shows a smoke back-layer, which occurred for rectangular dampers (RSD), a confinement velocity of 0.08 m/s and a Richardson number of 2.

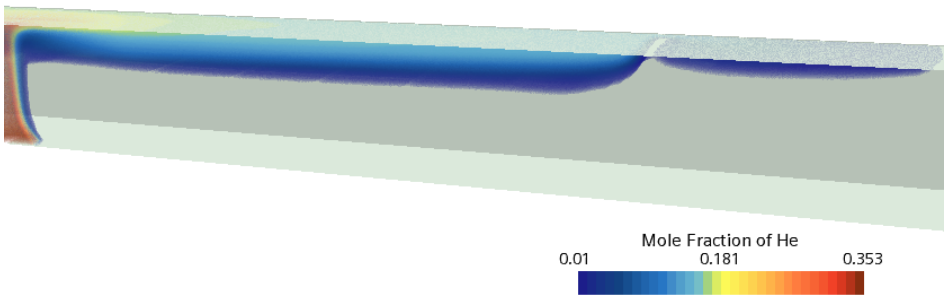

Figure 5: Configuration with rectangular dampers RSD, with a smoke back-layer occurring for U_{0cr} = 0.08 m/s and Γ_i = 2

Figure 6 shows confinement Froude number plotted against the Richardson number for each damper shape. Similarly to Figure 4, best fits of experimental results (solid bars) are given for the comparison. Dashed bars represent best fits of the simulation results. The regression was applied on Froude number obtained for $\Gamma_i > 4$ for the reason stated on section 3.1. However, unlike Figure 4, the confinement Froude number induced by centered square dampers (SSD PC) and rectangular dampers (RSD) do not seem to show any dependence at all on Γ_i (even for $\Gamma_i < 4$). Indicative 10% error bars have been added to simulation results.

It is first interesting to question the consistency between experimental and simulation results. All configurations show good correlations between experiment and simulation results. The reference configuration of sided square dampers (SSD_PS) lead to deviations within 10%. Its average deviation is about 6% (0.03 m/s). Centered square dampers (SSD PC) simulation results are on average 9.7% (0.02 m/s) lower than experimental results. Finally, rectangular dampers (RSD) are 17% lower on average than experimental results. However, in view of its smaller absolute value compared to other configurations, its absolute deviation remains very low (0.01 m/s).

Figure 6 show that the most common configuration (sided square dampers) is clearly the worst situation, leading to significantly higher confinement Froude number. Locating square dampers in the center of the ceiling allows to increase significantly the smoke exhaust effectiveness. The confinement Froude number is reduced by 52% compared to the reference configuration. Wide and slim rectangular dampers (transverse slits) are the most effective dampers. They allow to reduce the confinement Froude number by 84%. Experimental results led to quite similar benefits of the centered square dampers and rectangular dampers of respectively 44% and 80%.

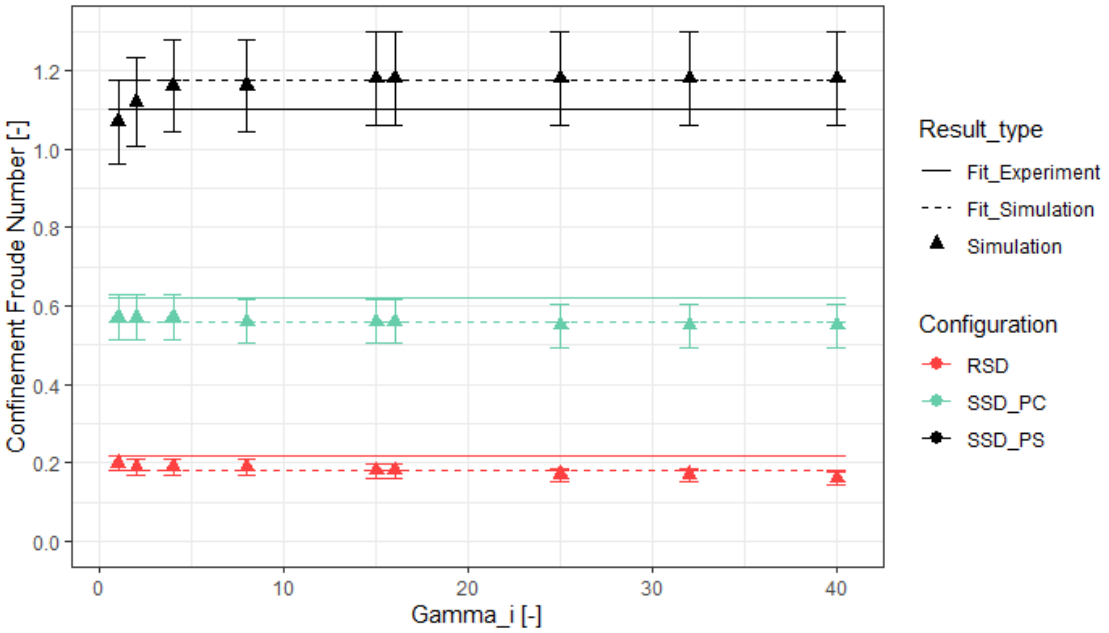

Figure 6: Critical Froude number plotted against the Richardson number for each damper shape

4. CONCLUSION

In this article, a reduced-scale tunnel CFD model was elaborated. It reproduced experiments that have previously been implemented. Those experiments questioned benefits of different configurations aiming at improving the robustness of the smoke exhaust by a longitudinal

and a transverse ventilation system. They showed that solid barriers attached to the ceiling appeared effective in reducing critical velocities involved in longitudinal ventilation systems. They also showed that the shape of dampers used in transverse ventilation systems has a significant influence on the confinement velocity.

Numerical results presented here allowed to verify significant improvements allowed by these passive geometrical optimizations. Large solid barriers led to a reduction of the critical velocity up to 33%, slightly weaker than experimental results that showed an even greater benefit of up to 45%. Regarding the transverse ventilation system, numerical and experimental results showed that narrow and wide rectangular dampers were way more efficient than usually installed square dampers. Both investigation techniques showed a reduction of the confinement velocity by around 80% compared to usually-installed sided square dampers. Locating the square damper in the center of the ceiling allows a reduction of around 50%.

The sensitivity of conclusion towards heat release rates has been assessed. As long as the buoyant source was buoyant enough (high Richardson number), the critical or the confinement Froude number was conserved for each HRR. It means that conclusions of the present paper are independent from the HRR.

The overall consistency between experimental and simulation results gives credit to those findings. Passive optimizations may, thus, have a great influence on the performance of ventilation systems. It is interesting to keep those findings in mind for the dimensioning and retrofitting of ventilation systems. It should however be taken into consideration that the implementation of those passive implementation may come with some technical difficulties that were not questioned in this paper. Also, vertical barriers proposed to improve the robustness of the longitudinal ventilation system may increase the wall friction. The energetic gain provided by the lower critical velocity as to be put in perspective of the energetic loss due to an increased wall friction. A following research will aim at questioning those results with the consideration of heat transfers among the tunnel's envelope.

5. REFERENCES

[1] F. Chaabat *et al.*, « The effects of solid barriers and blocks on the propagation of smoke within longitudinally ventilated tunnels », *Build. Environ.*, vol. 160, p. 106207, août 2019, doi: 10.1016/j.buildenv.2019.106207.

[2] F. Chaabat *et al.*, « Smoke control in tunnel with a transverse ventilation system: An experimental study », *Build. Environ.*, vol. 167, p. 106480, janv. 2020, doi: 10.1016/j.buildenv.2019.106480.

[3] L. Jiang, M. Creyssels, A. Mos, et P. Salizzoni, « Critical velocity in ventilated tunnels in the case of fire plumes and densimetric plumes », *Fire Saf. J.*, vol. 101, p. 53-62, oct. 2018, doi: 10.1016/j.firesaf.2018.09.001.

[4] P. Salizzoni, M. Creyssels, L. Jiang, A. Mos, R. Mehaddi, et O. Vauquelin, « Influence of source conditions and heat losses on the upwind back-layering flow in a longitudinally ventilated tunnel », *Int. J. Heat Mass Transf.*, n° 117, p. 143-153, 2018.

[5] G. R. Hunt et N. B. Kaye, « Lazy plumes », *J. Fluid Mech.*, vol. 533, p. 329-338, juin 2005, doi: https://doi.org/10.1017/S002211200500457X.